CrossMark

REVIEW

Advances in Imaging and Automated Quantification of Pulmonary Diseases in Non-neoplastic Diseases

Fernanda Balbinot[1,3,4] · Álvaro da Costa Batista Guedes[4] ·
Douglas Zaione Nascimento[4] · Juliana Fischman Zampieri[4] ·
Giordano Rafael Tronco Alves[2] · Edson Marchiori[2] ·
Adalberto Sperb Rubin[4] · Bruno Hochhegger[4]

Abstract Histological examination has always been the gold standard for the detection and quantification of lung remodeling. However, this method has some limitations regarding the invasiveness of tissue acquisition. Quantitative imaging methods enable the acquisition of valuable information on lung structure and function without the removal of tissue from the body; thus, they are useful for disease identification and follow-up. This article reviews the various quantitative imaging modalities used currently for the non-invasive study of chronic obstructive pulmonary disease, asthma, and interstitial lung diseases. Some promising computer-aided diagnosis methods are also described.

Keywords Pulmonary disease · Benign disease · Automated quantification · Quantitative method

Introduction

Pulmonary diseases lead to lung functional limitation by causing destruction or remodeling of the parenchyma and/or airway wall. Although histological examination is the gold standard for the assessment of lung remodeling, non-invasive methods enable the investigation of disease pathogenesis and changes over time, as well as the evaluation of new therapeutic interventions [1].

Quantitative imaging of the lung has been proven to be useful for disease identification and follow-up. Valuable information on lung structure can be obtained by quantitative computed tomography (CT) techniques, including high-resolution computed tomography (HRCT) and multidetector computed tomography (MDCT). To overcome the inter- and intraobserver variability inherent to radiologists' interpretation of CT images, the use of computer-aided diagnosis (CAD) systems has been improved since its introduction in the 1980s [2]. Increasing concerns about health risks related

✉ Fernanda Balbinot
  balbinotf@gmail.com

  Álvaro da Costa Batista Guedes
  alv_costa@hotmail.com

  Douglas Zaione Nascimento
  douglas.zn@bol.com.br

  Juliana Fischman Zampieri
  ju_zampieri@hotmail.com

  Giordano Rafael Tronco Alves
  grtalves@gmail.com

  Edson Marchiori
  edsonmarchiori@gmail.com

  Adalberto Sperb Rubin
  arubin@terra.com.br

  Bruno Hochhegger
  brunohochhegger@gmail.com

1 Federal University of Health Sciences of Porto Alegre, Porto Alegre, Brazil

2 Federal University of Rio de Janeiro, Rua Thomaz Cameron, 43, Valparaíso, Petrópolis, RJ 25685120, Brazil

3 Rua Coronel Vicente, 451, Centro, Porto Alegre, RS 90030041, Brazil

4 Irmandade Santa Casa de Misericórdia de Porto Alegre, LABIMED - Laboratório de Pesquisas em Imagens Médicas, Rua Prof. Annes Dias, 28, Centro, Porto Alegre, RS 90020090, Brazil

to the ionizing radiation needed to acquire CT images have led to the consideration of alternative methods, such as magnetic resonance imaging (MRI). MRI techniques, such as perfusion and diffusion weighting, allow the acquisition of morphological and functional lung images [3].The present article reviews the imaging methods and CAD systems available for the quantification of pulmonary changes in chronic obstructive pulmonary disease (COPD), asthma, and interstitial lung diseases (ILDs).

Chronic Obstructive Pulmonary Disease

COPD is characterized by irreversible airflow limitation, as demonstrated by a post-bronchodilator forced expiratory volume in the first second/forced vital capacity (FEV_1/ FVC) <70 % [4]. Airflow limitation in COPD is caused by a combination of factors, such as parenchymal lung destruction (emphysema) and loss or narrowing of small airways [5]. Because of its implications for the patient's response to therapeutic intervention, efforts have been made to evaluate the relative contributions of these two pathological processes to airflow limitation [6]. CT is currently the most widely available and precise imaging method for the characterization of COPD, although imaging techniques that do not require ionizing radiation are preferred for longitudinal monitoring.

Computed Tomography

Emphysema

Emphysema is characterized by abnormal, permanent enlargement of air spaces distal to the terminal bronchioles,

accompanied by the destruction of their walls [7]. On CT, emphysema appears as a set of areas with low attenuation values similar to those of air (Fig. 1). Currently, the reference standard for evaluation of the extent of disease on CT images is visual examination. This method, however, is subject to high degrees of inter- and intraobserver variability, and demands significant amounts of time and financial resources. Automated quantification of emphysema, on the other hand, provides objectivity and reproducibility [8].

On CT, the emphysematous lung is represented by image voxels with densities <−950 Hounsfield units (HU) (Fig. 2) [9]. The identification of all voxels with densities below this threshold is a process referred as density masking. The predetermined threshold can vary, however, depending on CT acquisition parameters, such as section thickness and reconstruction algorithm. Madani et al. [10] found that a threshold of −960 to −970 HU was suitable for the quantification of emphysema in continuous-volume MDCT datasets. Another approach—the percentile technique—consists of choosing a point on the percentile scale where the cumulative percentage of lung voxels is less than the cut-off value, and determining the corresponding attenuation value at that point. The 15th percentile has been proven to serve as a measure of lung destruction [1].

Numerous studies have assessed the usefulness of densitometric analysis in predicting clinically significant metrics, such as lung function. Although previous studies have shown that the extent of emphysema is not always correlated with the severity of airflow limitation [11, 12], the degree of emphysema measured by CT was found more recently to be correlated with levels of dyspnea, FEV_1, diffusing capacity of carbon monoxide, frequency of
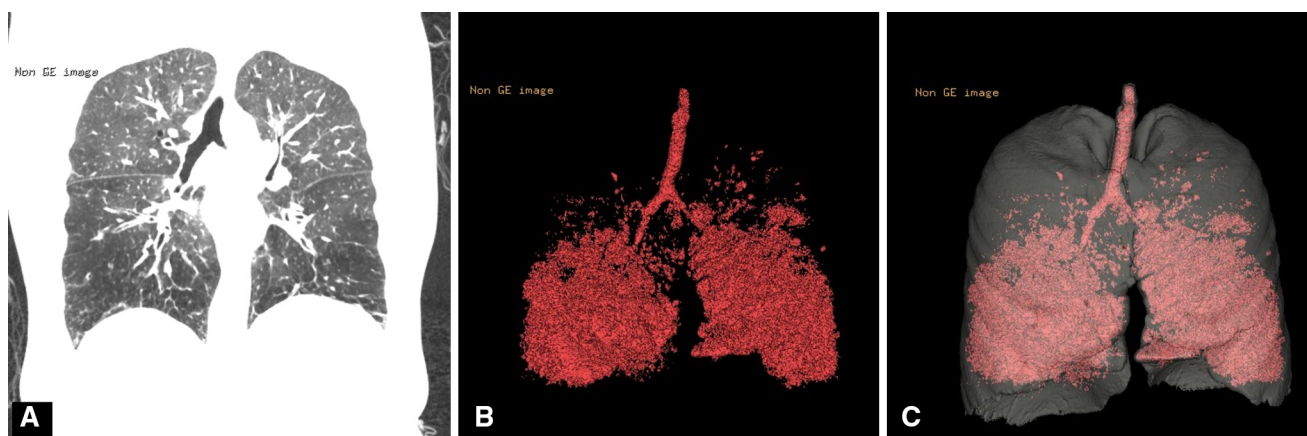

Fig. 1 45-year-old woman with alpha-1 antitrypsin deficiency. a Coronal CT image demonstrating extensive areas of low attenuation and bronchial wall thickening, mainly in the lower lobes. b Three-dimensional CT reconstruction demonstrating emphysematous areas (in red). c Three-dimensional CT reconstruction of total lung volume, overlaid with emphysematous areas (in red). Automated quantification revealed a total lung volume of 5.5 L and an emphysema index of 32.8 %, using a threshold of −950 HU

Fig. 2 65-year-old male smoker with dyspnea. **a** Axial CT image demonstrating extensive areas of emphysema. **b** Three-dimensional CT reconstruction demonstrating emphysematous areas (*in red*). **c** Three-dimensional CT reconstruction of total lung volume, overlaid with emphysematous areas (*in red*). Automated quantification revealed a total lung volume of 7.5 L, an estimated normal lung index of 52 %, and an emphysema index of 34.9 %, using a threshold of −950 HU
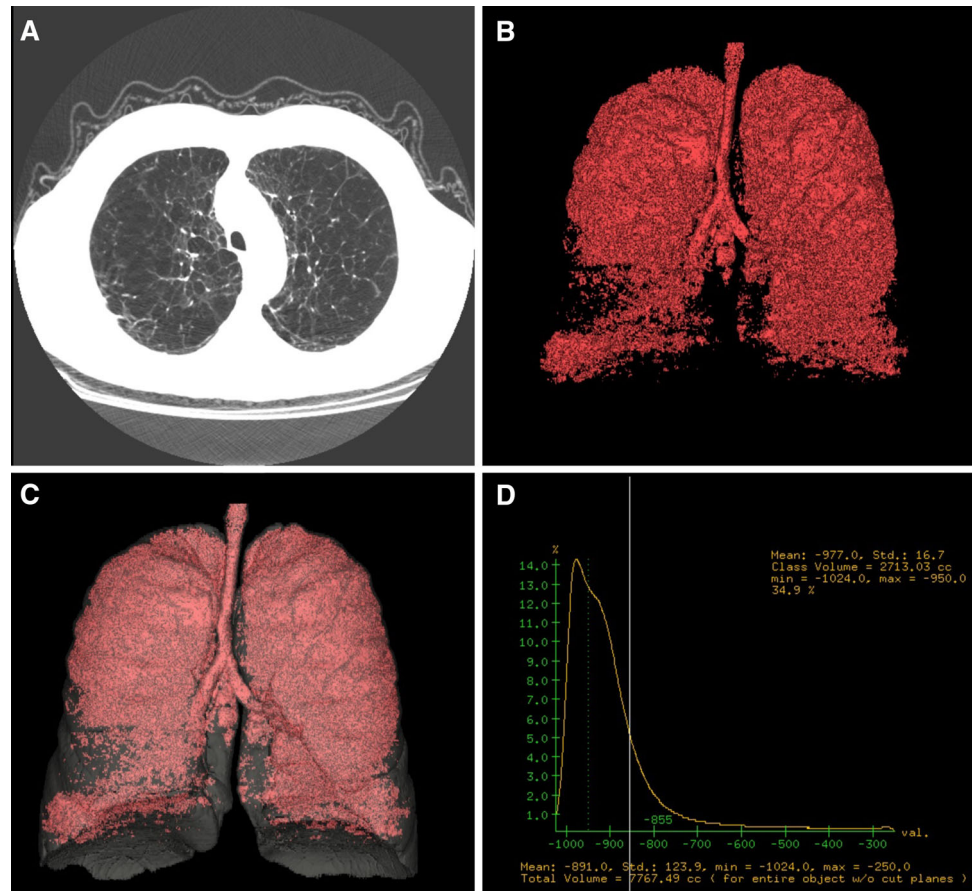
COPD exacerbations, the BODE index [composed of the body mass index (B), degree of airflow obstruction (O), level of functional dyspnea (D), and exercise capacity (E)], and quality of life scores [13]. Moreover, quantitative CT has been considered for the monitoring of emphysema progression and response to therapy [14].

However, the quantification of emphysema by automated methods has some limitations that cannot be ignored. First, quantification using density measures relies on a single threshold and independent voxel information. In addition, the level of inspiration during image acquisition, noise, scanner model, and reconstruction filter are all possible interfering variables [15–18]. Finally, another major limitation is the relative inability of these methods to provide information about the distribution of emphysematous changes, which differs according to emphysema subtype and should be taken into consideration to determine the appropriate therapeutic intervention [19].

In an attempt to overcome these problems, texture-based quantification of emphysema has been developed. Texture analysis involves the selection of a discrete region of interest in the lung and the assessment of several parameters in this constrained region, such as density and patterns of changes therein [1]. The simplest textural approach involves the identification of discrete and isolated zones of emphysema, and quantification of zones that are connected or clustered together [20].

Several CAD systems using texture analysis have been proposed to automate quantitative analysis and avoid intra- and inter-reader variability. The texture-based adaptive multiple feature method (AMFM), for example, uses mathematical formulations of the bright/dark pattern within the lung field to establish feature sets, which include measures such as mean lung density, kurtosis, skewness, entropy, run-length encoding, and stochastic fractal dimensions [7]. Uppaluri et al. [21] showed that the AMFM was more accurate than mean lung density for the discrimination of regional normal and emphysematous tissues. However, both methods correlated poorly with pulmonary function test results in the normal and emphysema groups.

Airway Measures

Small airway changes are considered to be among the earliest signs of COPD, preceding the development of emphysema [5]. The examination of air trapping on expiratory CT images is becoming quite popular for the assessment of small airway disease [22]. Air trapping,

which appears on these images as areas with less-than-normal increases in attenuation, is the retention of air distal to an obstruction (Fig. 3) [23]. The magnitude of change in lung attenuation after expiration is quantified using densitometric parameters, such as the difference between inspiratory and expiratory CT scans in the proportion of lung volume with a particular attenuation value (usually −856 HU), or the expiratory–inspiratory attenuation ratio (the ratio of mean lung attenuation on expiratory CT to that on inspiratory CT) [24].

Because pulmonary emphysema also corresponds to areas of reduced lung attenuation and is in itself a cause of air trapping, it acts as a confounding factor in the quantification of air trapping. In an effort to solve this problem, Matsuoka et al. [24] determined the attenuation threshold value for the detection and quantification of air trapping using paired inspiratory and expiratory volumetric MDCT images. The densitometric parameter of relative volume change using the threshold of −856 HU in impaired lungs was correlated closely with airway dysfunction in COPD, regardless of the degree of emphysema.

Several studies have shown that indexes derived from attenuation values on expiratory or paired expiratory and inspiratory CT images reflect airway obstruction in COPD. Lee et al. [2] demonstrated that expiratory lung density was correlated with the BODE index, and that CT and physiological measures of air trapping were correlated. Akira et al. [25] found that expiratory CT features were associated with pulmonary function in subjects with severe obstruction alone. Both studies showed that air trapping detection is enhanced when assessed on expiratory images, compared with inspiratory images.

One drawback of the use of expiratory CT is that it exposes the subject to extra radiation associated with a second CT examination. The radiation dose influences the signal-to-noise ratio: the noise level increases with decreasing dose [26]. Increased noise reduces the contrast between the airway wall and surrounding tissue, thereby reducing measurement accuracy. In addition to radiation exposure, the need for two CT acquisitions constitutes a disadvantage of the technique because expiration is difficult to obtain in patients with COPD. Quantification using expiratory CT also provides an assessment only of the consequences of pathological airway changes, and thus cannot be compared with pathological measures [27].

Magnetic Resonance Imaging

A substantial amount of research in lung imaging has focused on the development and application of inhaled and intravenous contrast agents to improve data collection [1]. The development of inhaled hyperpolarized helium-3 (^{3}He) and xenon-129 (^{129}Xe) contrast agents has overcome the low proton density issues inherent to lung tissues, which have limited image acquisition by conventional MRI [28]. In this approach, imaging typically takes place with the subject in breath-hold, 10–15 s after inhalation of a discrete volume of hyperpolarized xenon or helium gas. To date, hyperpolarized ^{3}He has been used widely in clinical research, as the gas remains in the airways without further interaction with the human body [29]. Hyperpolarized ^{3}He diffuses freely in the air at a rate of 0.88 cm^2/s until the diffusive movement is restricted by the alveolar boundaries. This restriction of movement is measurable by MRI and is known as the apparent diffusion coefficient (ADC), which is a direct representation of small airway size [30, 31] and is correlated closely with histology [32]. A high ADC indicates that the alveolar walls are further apart—due to alveolar destruction or acinar expansion—which is an early sign of emphysema [29]. The ADC was found to be more sensitive than spirometry and CT to mild emphysema in ex-smokers, and was related to symptoms and exercise limitation in these patients [33]. Importantly, the ADC has been shown to be sensitive to age [34–36],

Fig. 3 40-year-old woman with severe persistent asthma. **a** Airway wall thickness (WT) measurement from an axial CT image. **b** Coronal CT image and **c** three-dimensional CT reconstruction demonstrating air trapping areas

disease-related changes [37–39], and gravity-dependent compression of the lung [40].

More recently, MRI with ^{129}Xe has shed new light on lung function [41]. As xenon is lipid soluble, it has the additional advantage of being freely diffusible across the alveolar–capillary membrane, after which it is removed by capillary blood flow. This phenomenon allows the measurement of alveolar surface and alveolar blood-barrier thickness, which makes this technique a good option for the assessment of ventilation and perfusion [42].

Although MRI, particularly that performed with hyperpolarized gases, offers exciting possibilities for the measurement of alveolar dimensions, it currently cannot surpass HRCT in terms of speed, image contrast and content, and spatial resolution. In addition, a main disadvantage of MRI is that the contrast is exogenous and non-renewable. To overcome some of these limitations, other MRI techniques, such as the use of fluorine, ultrashort-echo-time pulse sequences, and oxygen-enhanced imaging, have been developed. These techniques may ultimately improve the treatment of patients with COPD.

Asthma

Asthma is characterized by chronic airway inflammation, which leads to airway remodeling and airway wall thickening [43]. Airway thickening involves the whole bronchial tree and results from mucosal infiltration by inflammatory cells; deposition of connective tissue on the extracellular matrix; and increases in muscle mass, mucus glands, and vessel area [44]. The severity of asthma is correlated with the degree of wall thickening, duration of the disease, and level of airflow obstruction [45–47]. The involvement of small airways, in particular, is largely responsible for irreversible airflow obstruction and increased airway responsiveness [48].

Airway dimensions in asthmatic patients have been assessed quantitatively by CT, which enables indirect measurement of airway remodeling using the total airway area, wall area, luminal area, and wall thickness of cross-sectional airways. Although HRCT may be used to assess structural changes in the asthmatic lung, MDCT is thought to be a better technique because it enables three-dimensional (3D) reconstruction of the bronchial tree for the measurement of more peripheral airways and segment-by-segment comparison among individuals [1]. Recently, Aysola et al. [45] used MDCT to demonstrate that airway walls are thicker in individuals with severe asthma than in those with mild or no asthma. The authors also demonstrated that thickening of airway walls is correlated positively with pathological measures of remodeling and the degree of airflow obstruction.

The analysis of smaller (luminal diameter < 1–2 mm) airway dimensions is beyond the spatial resolution limits of CT. Thus, some investigators have turned their attention to densitometric measurement on expiratory CT images. Measures of air trapping were shown to be correlated with clinical symptoms and response to therapy in asthmatic patients [49–52]. Busacker et al. [50] investigated whether air trapping was predictive of a more severe asthma phenotype. They defined air trapping as <-850 HU attenuation on expiratory CT images, and considered involvement of >9.66 % of the whole lung volume to be significant. They concluded that patients with the air trapping phenotype were more likely to have histories of asthma-related hospitalization and mechanical ventilation. They also noted some risk factors of this phenotype, such as a history of pneumonia, neutrophilic inflammation, and atopy.

Recently, the use of dynamic oxygen-enhanced MRI was compared with the use of quantitative CT for the assessment of clinical stage and pulmonary function change due to treatment in patients with asthma [53]. Correlations of dynamic oxygen-enhanced MRI with all parameters derived from pulmonary function tests—pre-therapeutic FEV_1/FVC, FEV_1, and the forced expiratory flow at 25–75 % of FVC ($FEF_{25-75\ \%}$)—were significantly better than those of quantitative CT. However, as inspiratory–expiratory CT was not tested, the potential of quantitative CT may have been underestimated.

Interstitial Lung Diseases

ILD encompasses more than 200 entities, including adult respiratory distress syndrome, sarcoidosis, non-specific interstitial pneumonia, and interstitial pulmonary fibrosis (IPF) [54]. HRCT is the current method of choice for ILD assessment. Several CAD tools have been developed for application to HRCT data. They involve texture-based voxel/pixel classification [55, 56], the assessment of first-order features based on density masks or histogram analysis [57, 58], and even sophisticated classification techniques such as continuous learning with physician-in-the-loop [59] or integrated methods [60, 61]. Although several CAD CT analytical methods have been proven to be useful for the assessment of disease severity and IPF progression, the NL % [which is defined as the percentage of the normally attenuated lung volume as defined from -950 to -701 HU (NL) to the volume of the whole lung (WL)] is significantly more useful than the percentages of predicted FVC and predicted diffusing capacity of the lungs for carbon monoxide for this purpose [62].

CAD schemes enable not only the quantification of disease extent, but also estimation of the contribution of each specific abnormality—ground-glass opacity,

reticulation, and honeycombing—to disease progression (Figs. 4, 5) [63]. Maldonado et al. [64] explored the use of Computer-Aided Lung Informatics for Pathology Evaluation and Rating (CALIPER) to assess baseline and follow-up HRCT images in patients with IPF. They found that the volume of reticular densities, total volume of interstitial abnormalities, and percent total of interstitial abnormalities were predictive of survival after a median follow-up period of 2.4 years. However, the authors noted that misclassification of abnormalities with similar density but different morphologies may occur with CALIPER.

Traditionally, technical limitations of CT scanners required that HRCT imaging protocols involve the acquisition of non-contiguous thin slices (1 mm) every 10–20 mm, which limited the ability to cover the entire lung parenchyma volume and restricted anatomic

Fig. 4 54-year-old woman with idiopathic pulmonary fibrosis. a Axial CT image demonstrating areas of ground-glass opacity, septal thickening, and honeycombing bilaterally in the cortical zones of the lower lobes. b Coronal CT image depicting the prevalence of these findings in the lower lobes. c Three-dimensional CT reconstruction of the total lung volume. d Three-dimensional CT reconstruction of interstitial lung disease volumes. Automated quantification revealed a total lung volume of 3.2 L, an estimated normal lung index of 32 %, and an interstitial lung disease index of 22 %
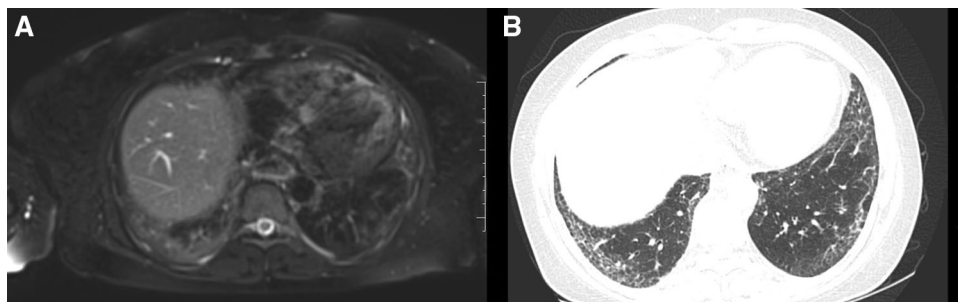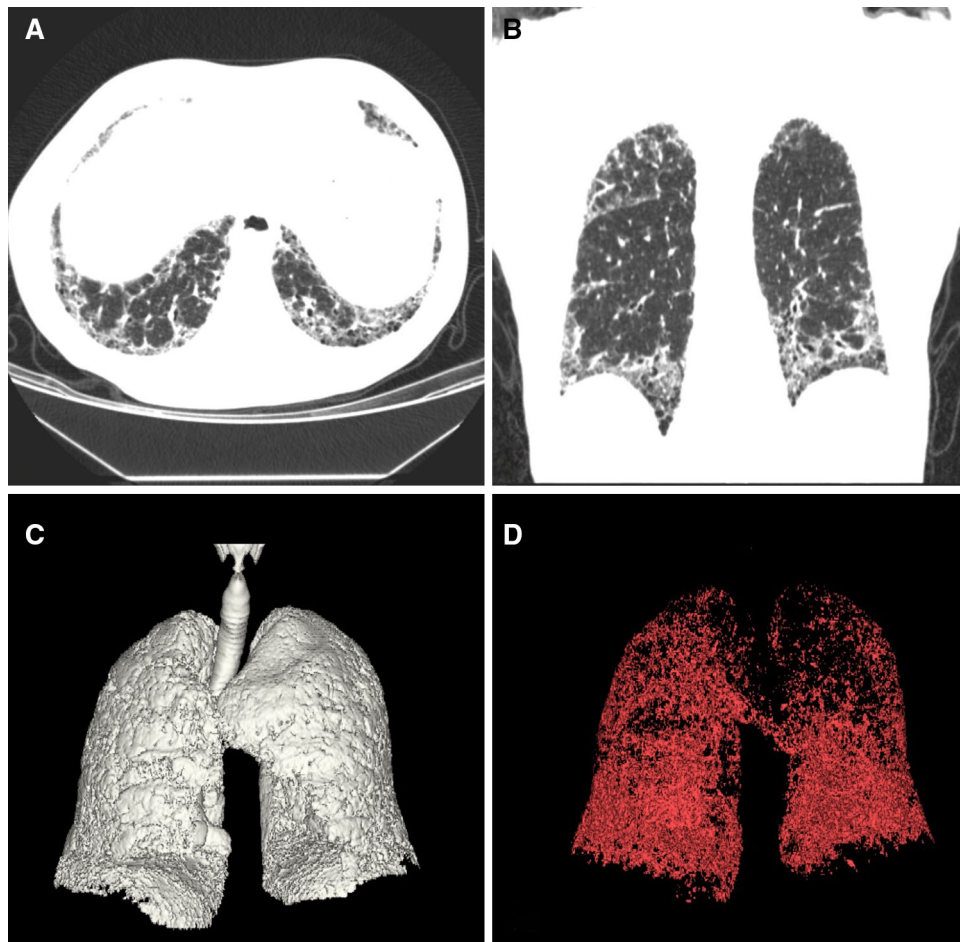

Fig. 5 42-year-old man with scleroderma. a Axial CT image demonstrating extensive areas of ground-glass opacity and septal thickening bilaterally in the cortical zones of the lower lobes. b Axial T2-weighted MR image demonstrating extensive areas of hyperintensity unilaterally in the cortical zone of the right lower lobe, suggesting the presence of a non-inflammatory lesion at this site

comparability in follow-up studies [65]. MDCT has enabled the performance of isotropic high-resolution 3D scans of the entire chest in a single breath-hold. Some CAD systems have been developed for application to MDCT image data, which enables the volumetric quantification of disease extent [56, 60, 61]. Recently, Colombi et al. [58] found that values of the 40th and the 80th percentiles on MDCT attenuation frequency histograms were promising parameters for the monitoring of disease extent in patients with IPF. The 40th percentile appears to reflect the change in the overall extent of lung abnormalities, notably the ground-glass pattern, and the 80th percentile was found to reveal the course of reticular opacities.

Although CT is the method of choice for the evaluation of patients with suspected or known ILD, some studies have assessed the use of alternative imaging methods, such as MRI, for disease characterization and follow-up. Buzan et al. [66] evaluated the use of lung T2 mapping for the quantitative characterization and differentiation of normal tissue, ground-glass opacity, reticulation, and honeycombing in patients with stable usual interstitial pneumonia or non-specific interstitial pneumonia. They found significant differences in T2 relaxation between normal and pathological areas, and among ground-glass opacities, reticulation, and honeycombing. These findings indicate that T2 relaxation in lung remodeling can reflect the amount of fibrosis burden and may allow for the monitoring of progression and response to therapy in ILD. The ability of MRI to depict pulmonary abnormalities suggestive of pneumonia was compared with that of HRCT in patients with neutropenia [66]. The sensitivity of MR images for the detection of pneumonia was 95 %, the specificity was 88 %, and the positive and negative predictive values were 95 and 88 %, respectively. After proper adjustment, the description of lesion location and distribution did not differ significantly between modalities. Ground-glass opacities were detected by CT in 14 patients and by MRI in the same 14 patients as well as 2 others. Of these two cases additionally detected by MRI, one was misdiagnosed as a result of blurring artifacts; in the other case, CT performed 3 days later showed a ground-glass area in the location depicted previously on MRI. These findings suggest that MRI has greater sensitivity than CT in this context. Few published studies have directly compared pulmonary CT and MRI for the assessment of ILD; thus, this topic requires further investigation.

Conclusion

CT remains the method of choice for quantitative assessment of the lung. However, other imaging modalities and CAD systems are being developed and improved to enable the best quantitative studies of lung anatomy and function. When properly controlled, these methods can produce reliable and valuable data for the analysis of lung structure, which can be used to study the pathogenesis of diseases and the effects of therapeutic interventions.

Compliance with Ethical Standards

Conflict of Interest All authors declare that they have no conflict of interest.

References

1. Washko GR, Parraga G, Coxson HO (2012) Quantitative pulmonary imaging using computed tomography and magnetic resonance imaging. Respirology 17:432–444
2. Lee YK, Oh YM, Lee JH et al (2008) Quantitative assessment of emphysema, air trapping, and airway thickening on computed tomography. Lung 186:157–165
3. Henzler T, Schmid-Bindert G, Schoenberg SO et al (2010) Diffusion and perfusion MRI of the lung and mediastinum. Eur J Radiol 76:329–336
4. Pauwels RA, Buist AS, Calverley PM et al (2001) Global Strategy for the diagnosis, management, and prevention of chronic obstructive pulmonary disease. NHLBI/WHO global initiative for chronic obstructive lung disease (GOLD) workshop summary. Am J Respir Crit Care Med 163:1256–1276
5. McDonough JE, Yuan R, Suzuki M et al (2011) Small-airway obstruction and emphysema in chronic obstructive pulmonary disease. N Engl J Med 365:1567–1575
6. Tho NV, Ryujin Y, Ogawa E et al (2015) Relative contributions of emphysema and airway remodelling to airflow limitation in COPD: consistent results from two cohorts. Respirology 20:594–601
7. Hoffman EA, Reinhardt JM, Sonka M et al (2003) Characterization of the interstitial lung diseases via density-based and texture-based analysis of computed tomography images of lung structure and function. Acad Radiol 10:1104–1118
8. Ginsburg SB, Lynch DA, Bowler RP et al (2012) Automated texture-based quantification of centrilobular nodularity and centrilobular emphysema in chest CT images. Acad Radiol 19:1241–1251
9. Milne S, King GG (2014) Advanced imaging in COPD: insights into pulmonary pathophysiology. J Thorac Dis 6:1570–1585
10. Madani A, Zanen J, de Maertelaer V et al (2006) Pulmonary emphysema: objective quantification at multi-detector row CT—comparison with macroscopic and microscopic morphometry. Radiology 238:1036–1043
11. Gelb AF, Schein M, Kuei J et al (1993) Limited contribution of emphysema in advanced chronic obstructive pulmonary disease. Am Rev Respir Dis 147:1157–1161
12. Hogg JC, Wright JL, Wiggs BR et al (1994) Lung structure and function in cigarette smokers. Thorax 49:473–478
13. Martinez CH, Chen YH, Westgate PM et al (2012) Relationship between quantitative CT metrics and health status and BODE in chronic obstructive pulmonary disease. Thorax 67:399–406
14. Coxson HO, Dirksen A, Edwards LD et al (2013) The presence and progression of emphysema in COPD as determined by CT scanning and biomarker expression: a prospective analysis from the ECLIPSE study. Lancet Respir Med 1:129–136
15. Boedeker KL, McNitt-Gray MF, Rogers SR et al (2004) Emphysema: effect of reconstruction algorithm on CT imaging measures. Radiology 232:295–301

16. Stoel BC, Bakker ME, Stolk J et al (2004) Comparison of the sensitivities of 5 different computed tomography scanners for the assessment of the progression of pulmonary emphysema: a phantom study. Invest Radiol 39:1–7

17. Sieren JP, Newell JD, Judy PF et al (2012) Reference standard and statistical model for intersite and temporal comparisons of CT attenuation in a multicenter quantitative lung study. Med Phys 39:5757–5767

18. Bakker ME, Stolk J, Putter H, Shaker SB et al (2005) Variability in densitometric assessment of pulmonary emphysema with computed tomography. Invest Radiol 40:777–783

19. Fishman A, Martinez F, Naunheim K et al (2003) National Emphysema Treatment Trial Research Group. A randomized trial comparing lung-volume-reduction surgery with medical therapy for severe emphysema. N Engl J Med 348:2059–2073

20. Mishima M, Hirai T, Itoh H et al (1999) Complexity of terminal airspace geometry assessed by lung computed tomography in normal subjects and patients with chronic obstructive pulmonary disease. Proc Natl Acad Sci USA 96:8829–8834

21. Uppaluri R, Mitsa T, Sonka M et al (1997) Quantification of pulmonary emphysema from lung computed tomography images. Am J Respir Crit Care Med 156:248–254

22. Coxson HO, Lam S (2009) Quantitative assessment of the airway wall using computed tomography and optical coherence tomography. Proc Am Thorac Soc 6:439–443

23. Hansell DM, Bankier AA, MacMahon H et al (2008) Fleischner society: glossary of terms for thoracic imaging. Radiology 246:697–722

24. Matsuoka S, Kurihara Y, Yagihashi K et al (2008) Quantitative assessment of air trapping in chronic obstructive pulmonary disease using inspiratory and expiratory volumetric MDCT. AJR Am J Roentgenol 190:762–769

25. Akira M, Toyokawa K, Inoue Y et al (2009) Quantitative CT in chronic obstructive pulmonary disease: inspiratory and expiratory assessment. AJR Am J Roentgenol 192:267–272

26. Madani A, De Maertelaer V, Zanen J et al (2007) Pulmonary emphysema: radiation dose and section thickness at multidetector CT quantification—comparison with macroscopic and microscopic morphometry. Radiology 243:250–257

27. Hackx M, Bankier AA, Gevenois PA (2012) Chronic obstructive pulmonary disease: CT quantification of airways disease. Radiology 265:34–48

28. Fain S, Schiebler ML, McCormack DG et al (2010) Imaging of lung function using hyperpolarized helium-3 magnetic resonance imaging: review of current and emerging translational methods and applications. J Magn Reson Imaging 32:1398–1408

29. van Beek EJR, Hoffman EA (2008) Functional imaging: CT and MRI. Clin Chest Med 29:195–216

30. de Lange EE, Mugler JP, Brookeman JR et al (1999) Lung air spaces: MR imaging evaluation with hyperpolarized 3He gas. Radiology 210:851–857

31. Kauczor HU, Ebert M, Kreitner KF et al (1997) Imaging of the lungs using 3He MRI: preliminary clinical experience in 18 patients with and without lung disease. J Magn Reson Imaging 7:538–543

32. Woods JC, Choong CK, Yablonskiy DA et al (2006) Hyperpolarized 3He diffusion MRI and histology in pulmonary emphysema. Magn Reson Med 56:1293–1300

33. Kirby M, Owrangi A, Svenningsen S et al (2013) On the role of abnormal DL(CO) in ex-smokers without airflow limitation: symptoms, exercise capacity and hyperpolarised helium-3 MRI. Thorax 68:752–759

34. Fain SB, Altes TA, Panth SR et al (2005) Detection of age-dependent changes in healthy adult lungs with diffusion-weighted 3He MRI. Acad Radiol 12:1385–1393

35. Altes TA, Mata J, de Lange EE et al (2006) Assessment of lung development using hyperpolarized helium-3 diffusion MR imaging. J Magn Reson Imaging 24:1277–1283

36. Parraga G, Mathew L, Etemad-Rezai R et al (2008) Hyperpolarized 3He magnetic resonance imaging of ventilation defects in healthy elderly volunteers: initial findings at 3.0. Tesla Acad Radiol 15:776–785

37. Salerno M, de Lange EE, Altes TA et al (2002) Emphysema: hyperpolarized helium 3 diffusion MR imaging of the lungs compared with spirometric indexes—initial experience. Radiology 222:252–260

38. Swift AJ, Wild JM, Fichele S et al (2005) Emphysematous changes and normal variation in smokers and COPD patients using diffusion 3He MRI. Eur J Radiol 54:352–358

39. van Beek EJ, Dahmen AM, Stavngaard T et al (2009) Hyperpolarised 3-He MRI vs HRCT in COPD and normal volunteers—PHIL trial. Eur Respir J 34:1311–1321

40. Fichele S, Woodhouse N, Said Z et al (2004) MRI of Helium-3 Gas in healthy lungs: posture related variations of alveolar size. J Magn Reson Imaging 20:331–335

41. Patz S, Muradyan I, Hrovat MI et al (2011) Diffusion of hyperpolarized 129Xe in the lung: simplified model of 129Xe septal uptake and experimental results. New J Phys 13:015009

42. Patz S, Muradian I, Hrovat MI et al (2008) Human pulmonary imaging and spectroscopy with hyperpolarized 129-Xe at 0.2T. Radiology 15:713–727

43. Niimi A, Matsumoto H, Takemura M et al (2004) Clinical assessment of airway remodeling in asthma: utility of computed tomography. Clin Rev Allergy Immunol 27:45–58

44. Bousquet J, Chanez P, Lacoste JY et al (1992) Asthma: a disease remodeling the airways. Allergy 47:3–11

45. Aysola RS, Hoffman EA, Gierada D et al (2008) Airway remodeling measured by multidetector CT is increased in severe asthma and correlates with pathology. Chest 134:1183–1191

46. Niimi A, Matsumoto H, Amitani R et al (2004) Effect of short-term treatment with inhaled corticosteroid on airway wall thickening in asthma. Am J Med 116:725–731

47. Kasahara K, Shiba K, Ozawa T et al (2002) Correlation between the bronchial subepithelial layer and whole airway wall thickness in patients with asthma. Thorax 57:242–246

48. Gono H, Fujimoto K, Kawakami S et al (2003) Evaluation of airway wall thickness and air trapping by HRCT in asymptomatic asthma. Eur Respir J 22:965–971

49. Busacker A, Newell JD Jr, Keefe T et al (2009) A multivariate analysis of risk factors for the air-trapping asthmatic phenotype as measured by quantitative CT analysis. Chest 135:48–56

50. Zeidler MR, Kleerup EC, Goldin JG et al (2006) Montelukast improves regional air-trapping due to small airways obstruction in asthma. Eur Respir J 27:307–315

51. Lee E, Seo JB, Lee HJ et al (2015) Quantitative assessment of global and regional air trappings using non-rigid registration and regional specific volume change of inspiratory/expiratory CT scans: studies on healthy volunteers and asthmatics. Korean J Radiol 16:632–640

52. Ohno Y, Nishio M, Koyama H et al (2014) Asthma: comparison of dynamic oxygen-enhanced MR imaging and quantitative thin-section CT for evaluation of clinical treatment. Radiology 273:907–916

53. Ryu JH, Colby TV, Hartman TE et al (2001) Smoking-related interstitial lung diseases: a concise review. Eur Resp J 17:122–132

54. Yoon RG, Seo JB, Kim N et al (2013) Quantitative assessment of change in regional disease patterns on serial HRCT of fibrotic interstitial pneumonia with texture-based automated quantification system. Eur Radiol 23:692–701

55. Korfiatis PD, Karahaliou AN, Kazantzi AD et al (2010) Texture-based identification and characterization of interstitial pneumonia patterns in lung multidetector CT. IEEE Trans Inf Technol Biomed 14:675–680

56. Hartley PG, Galvin JR, Hunninghake GW et al (1994) High-resolution CT-derived measures of lung density are valid indexes of interstitial lung disease. J Appl Physiol 76:271–277

57. Colombi D, Dinkel J, Weinheimer O et al (2015) Visual vs fully automatic histogram-based assessment of idiopathic pulmonary fibrosis (IPF) progression using sequential multidetector computed tomography (MDCT). PLoS One 10:e0130653

58. Shyu CR, Brodley CE, Kak AC et al (1999) Assert: a physician-in-the-loop content-based retrieval system for HRCT image databases. Comput Vis Image Underst 75:111–132

59. Zavaletta VA, Bartholmai BJ, Robb RA (2007) High resolution multidetector CT-aided tissue analysis and quantification of lung fibrosis. Acad Radiol 14:772–787

60. Xu Y, van Beek EJ, Hwanjo Y et al (2006) Computer-aided classification of interstitial lung diseases via MDCT: 3D adaptive multiple feature method (3D AMFM). Acad Radiol 13:969–978

61. Ohkubo H, Kanemitsu Y, Uemura T et al (2016) Normal lung quantification in usual interstitial pneumonia pattern: the impact of threshold-based volumetric ct analysis for the staging of idiopathic pulmonary fibrosis. PLoS One. doi:10.1371/journal.pone.0152505

62. Gruden JF, Panse PM, Leslie KO et al (2013) UIP diagnosed at surgical lung biopsy, 2000–2009: HRCT patterns and proposed classification system. AJR Am J Roentgenol 200:W458–W467

63. Maldonado F, Moua T, Rajagopalan S et al (2014) Automated quantification of radiological patterns predicts survival in idiopathic pulmonary fibrosis. Eur Respir J 43:204–212

64. Uchiyama Y, Katsuragawa S, Abe H et al (2003) Quantitative computerized analysis of diffuse lung disease in high-resolution computed tomography. Med Phys 30:2440–2454

65. Buzan MTA, Eichinger M, Kreuter M et al (2015) T2 mapping of CT remodelling patterns in interstitial lung disease. Eur Radiol 25:3167–3174

66. Eibel R, Herzog P, Dietrich O et al (2006) Pulmonary abnormalities in immunocompromised patients: comparative detection with parallel acquisition MR imaging and thin-section helical CT. Radiology 241:880–891